Performance of low height railway noise barriers

João Lázaro [1], Matheus Pereira [1],Pedro Alves Costa [1], Luís Godinho[2]

[1]Department of Civil Engineering, University of Porto, Construct, Porto, Portugal
(jlazaro@fe.up.pt, pacosta@fe.up.pt, matheus.pereira@eac.ufsm.br)

[2]Department of Civil Engineering, University of Coimbra, ISISE, Coimbra, Portugal
(lgodinho@dec.uc.pt)

Abstract

Although railway system is the most sustainable mode of transport, with the lowest energy consumption, the noise induced by rail traffic in urban regions is a significant drawback. Mitigation of railway noise can be performed by different solutions, namely by the implementation of acoustic barriers. Although they offer a significant reduction in noise levels, their height makes people feel enclosed. Therefore, in the case of the railway infrastructure, the solution to the problem may lie in the use of barriers with a lower height placed close to the railway track.

The purpose of this paper is to illustrate the development of a barrier solution to be used in a railway context through numerical modelling with BEM. The solutions developed were placed close to the track and have a low height (approximately 0.8 m above the rail head). The geometry was defined so as to direct the energy back to the track to take advantage of the acoustic properties of the ballast. The addition of a porous granular material on the inner face of the barrier allows the control of reflections between the vehicle body and the barrier, increasing its acoustic efficiency.

Keywords: Railway noise, Low height acoustic barrier, Acoustic efficiency.

1   Introduction

Rail transport is the most sustainable mode of transport, with the lowest energy consumption and carbon footprint compared to any other mode of transport.

A report by the European Environment Agency (EEA) [1], points that on a European level, rail noise is the second dominant source of noise, with a trend of increasing numbers of people being exposed in the coming decades according to [2]. Rail noise mitigation measures are applied in three different locations depending on the level of mitigation [3]. Usually, the most common solutions are used at the level of the propagation path of sound waves, in this case acoustic barriers.

Acoustic barriers have been widely adopted in the context of noise mitigation; however, due to their height (usually 3 m to 4 m high), these solutions face criticism from the population living and transiting in the proximity of railway lines. The reason for that criticism lies in the feeling of entrapment caused by the barriers, affecting the field of vision, loss of natural light and normal air circulation [4]. In order to tackle this problem, new solutions, such as the one presented in this paper, have been studied by different researchers.

The advantage of low height noise barriers is related to the positioning of the barrier. As the noise formation mechanisms are located mainly at the rail level [5], placing the barrier in a position close to the track allows the propagation of sound waves to be interrupted near the source without presenting itself as an obstacle, as happens with the usual barriers. With this in mind, several authors have worked on this issue in order to develop a solution to mitigate the noise levels associated with rail traffic [6, 7].

In order to increase the efficiency of the barrier, in this case to control reflections between the vehicle body and the barrier, an absorptive treatment is required. For this purpose the use of porous concrete made with light and sustainable consolidated granular materials, is of special interest from the point of view of sustainability and resistance to external actions [8-10]. Research on the equivalent fluid representation of porous concrete made with expanded clay has been shown to be relevant in the scientific community [9, 10]. In this work, the numerical modelling of railway scenarios is essential for the construction of the low height acoustic barrier. The Boundary Element Method (BEM) is widely used to solve acoustic problems [11, 12] and can be an excellent option for modelling the effect of mitigation measures. The numerical model allows the incorporation of purely reflective boundaries and the modelling of wave propagation in different fluid media.

The structure of the paper is as follows: The section 2 presents the experimental characterization of railroad noise. The section 3 summarizes the experimental procedure used to characterize porous concrete samples, allowing the representation of fluid equivalence theory. Section 4 presents the numerical formulation of the BEM used to model the described problem. Section 5 presents the strategy used to define the barrier geometry. Section 6 outlines the main results obtained from the studies performed. Finally, section 7 summarizes the main conclusions of this work.

2   Railway noise characterization

Noise induced by rail traffic comes from various sources and has many different characteristics. Despite the various components of railway noise, the most predominant noise is the result of wheel-rail interaction, influenced by the speed of movement of vehicles.
In order to identify the main frequency content, an experimental characterization campaign was carried out, in which the signal acquisition was done using four Behringer microphones type ECM 8000, connected to a Focusrite Sclarett 4Pre USB for signal acquisition.
The placement of the microphones was set to allow the acquisition of the noise at the closest possible location to the source, and at successive greater distances from the source, thus allowing the propagation of the sound waves to be studied in a comprehensive manner.
The Figure 1 shows the configuration used for the measurement, with the distance between microphones and the position relative to the track.
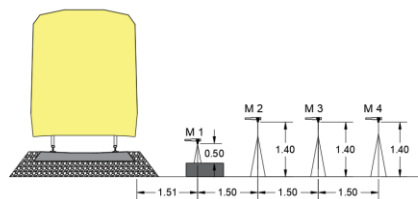

Figure 1 - Experimental setup configuration.

The sound pressure levels shown in Figure 2 were collected on a ballasted track site with trainsets running at different speeds (84 km/h and 78 km/h respectively). By analysing the one-third octave bands presented, it is concluded that the most prevalent frequency content responsible for the highest noise levels lies between 200 Hz and 4000 Hz, i.e. the frequency interval between the two discontinuous black lines in each of the third octave bands. This information has been the basis for the numerical modelling presented later in this paper, allowing the definition of the frequency range and content that needs to be mitigated by the noise barrier.
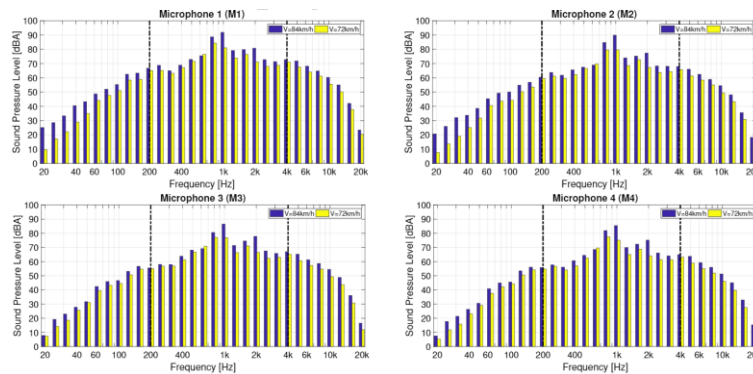
Figure 2 - Records of measured sound pressure levels; in blue a vehicle operating at 84 km/h; in yellow a vehicle operating at 72 km/h.

3   Experimental characterization of porous concrete

Granular elements used in the construction of porous concrete are generally distributed differently from fibres, following a log-normal pore distribution, resulting in lower porosity and higher tortuosity. Therefore, the absorption coefficient of these materials depends on the pore size, porosity, tortuosity and sample thickness of the material. The porous concrete samples were produced using expanded clay aggregates with a particle size of 0-2 mm. Six samples were prepared, where all samples are 10.1 cm in diameter and 4, 6 and 8 cm thick. The proportions between the components of the materials by weight (kg) are shown in Table 1.

Table 1 – Material proportions in weight (kg) of the produced samples

Grain size (mm)	Aggregate (%)	Cement (%)	Water (%)
0-2	43.96	37.36	18.68

An experimental procedure based on the use of an impedance tube was used to characterize the normal incidence acoustic properties of the porous concrete samples. As described in ISO 10534-2 [13], these properties can be obtained from the transfer function between two microphones. To obtain the intrinsic acoustic properties of the porous concrete samples, the Two-Cavity Method proposed by Utsuno [14] was used. Figure 3-a) shows the porous concrete samples and Figure 3-b) sound absorption curves between samples with different thickness. Each curve corresponds to the average between the two samples of same thickness, respectively, 4, 6 and 8 cm. It is observed that the increase of the thickness produces a shift in the sound absorption coefficient curve towards low frequencies.

a)
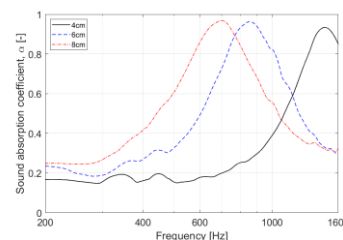
b)

Figure 3 - Sound absorption behavior of porous concrete. (a) Porous concrete built samples. (b) Average of the sound absorption coefficient for three different thicknesses: 4, 6, and 8 cm.

To predict the acoustic behaviour of porous concrete with different thickness and to represent these materials as the fluid-equivalent theory the Horoshenkov and Swift model is performed. This model consider four

macroscopic parameters to determine the acoustic behaviour, to list: air flow resistivity, σ, open porosity, ϕ, tortuosity, α_∞, and the standard deviation of the pore size, σ_p.

The inverse technique was performed using a genetic algorithm in which the objective function was based on the quadratic sum of errors between the analytical and experimental data, along a frequency range.

Figure 4 shows a comparison between the complex properties using the presented macroscopic parameters and those experimentally obtained through the Two-Cavity method for a sample with 4 cm. As observed in [15] an excellent agreement can be observed between the experimental data and the semi phenomenological prediction, allowing to represent and predict the porous concrete behaviour for different samples thicknesses and geometries.
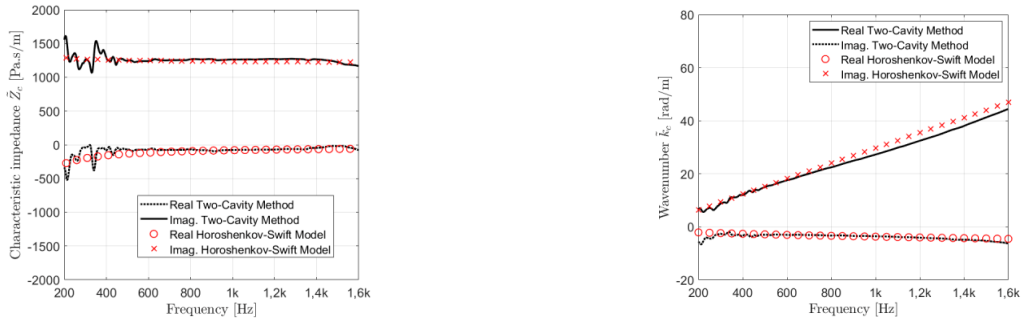

Figure 4 - Comparison between the experimental characterization and the semi phenomenological representation. (a) Characteristic impedance, Z_c; (b) Wavenumber, k_c. (Adapted from [15]}).

4   System modelling

The Boundary Element Method, BEM, allows the analysis of complex geometries without the need to describe the entire propagation medium, allows solving problems with both infinite and limited domains. The solution to the problem involves solving the Helmholtz equation, where *p* is the acoustic pressure and *k* is the wave number.

$$\nabla^2 p + k^2 p = \delta(r_1 - r_0).$$
(1)

Solving the equation (1) is done by approximating the solutions for each boundary element. The numerical method involves defining a virtual source P, one of the boundary elements, and integrating the other boundary elements, Q. This operation is performed for all boundary elements, thus creating a system of equations N, where N is equal to the number of boundary elements. The solution is obtained as the sum of the solution of the integrals for each collocation point. Typically, the matrix formulation is used as the preferred means of presenting the boundary element method [16],

$$Cp - Hp = i\rho_0 \omega G v + p_{inc.}$$
(2)

Where p and v, are the acoustic quantities to be calculated, pressure and velocity of the particles according to the normal to the surface and p_{inc} is the free-field acoustic pressure due to a source located in the domain.

The matrices **G** and **H** are complete matrices and contain the Green solutions for all boundary points. Finally, **C** is a diagonal matrix whose values depend on the placement point.

In order to represent the porous materials that must be placed in the barrier and study in this paper, it is necessary to include the simulation of porous materials as fluid equivalents. It is necessary to define each media and ensure coupling between the pressures and the normal velocity at the interfaces. The systematisation of this problem involves defining the equations presented in equation (2) for each propagation domain and their boundaries valid for both the external domain, $\Omega_{exterior}$, and the internal domain,

Ω_i, as illustrated in Figure 5. The coupling between domains is done by ensuring the continuity of the pressure and particle velocity conditions at the shared boundaries of the domains [17].
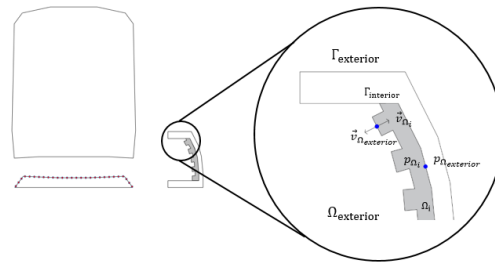

Figure 5 - Representation of the coupled interior/exterior problem.

Once the acoustic variables at the defined boundaries are known, the acoustic pressure at the external receivers, p^T, is equal to the sum of the incident field acoustic pressure, p_{inc}, and the acoustic pressure resulting from the interaction of the boundaries with the acoustic medium, p^S, as shown in Equation 3.

$$p^t = p_{inc} + p^S.$$

(3)

5   Methodology

The following section is intended to describe the methodology used to achieve the final low height acoustic barrier solution.

The diagram in Figure 6 summarizes the main steps that were necessary, from the way the barrier geometry was designed to the study of ways to improve its acoustic efficiency.
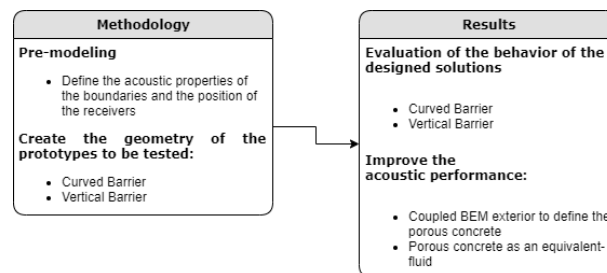

Figure 6 - Schematic representation of the methodology and results.

The application of the BEM 2D model makes it possible to calculate the effect of acoustic barriers in a railway environment. In order to accurately describe the acoustic conditions of the modeled boundaries a purely reflective condition was defined for the vehicle and part of the acoustic barrier, which means that the particle velocity is zero. However, for the track (indicated in the figure as red dots) an impedance condition was prescribed, which allows the acoustic absorption coefficient of the ballast to be considered. Thus, to consider the absorption capacity of the ballast, based on the work developed by Broadbent [18], which presents the acoustic absorption coefficient for a 17 cm ballast layer, the surface impedance of the ballast was calculated.

The information collected from Metro do Porto, SA, allowed the modeling of the elements that are part of the railway context, thus getting as close as possible to the real scenario. This information allowed us to define the distance between the track and the barrier, setting it at 1.225 m. As shown in the diagram above,

5

the design process of the barrier led to define a curved solution in order to take advantage of the acoustic properties of the ballast, sending as much energy back to the track as possible.

The construction of the curved geometry of the barrier was done using the simulation of the propagation of a sound wave in the time domain, in order to match the inner face of the barrier to the wave front. The Figure 7-a) presents the time domain simulation of the acoustic wave at the location where the barrier will be placed, also representing a low height curved noise barrier with the inner face coinciding with the wave front. As a result, the final geometry of the barrier is shown in Figure 7-b).

a)   b)

Figure 7 - (a) Schematic representation of the wave front and the designed barrier; (b) Representation of the main dimensions of the final barrier.

The position of receivers has been defined considering the circulation of pedestrians alongside the track (in the case of the lower receivers) and sensible buildings (in the case of the higher receivers).

Figure 8 presents the grid of external receivers (black dots) used in the studies presented in the following sections. As can be seen, the grid extends about 7 meters in length and 5 meters in height, incorporating the receivers mentioned above.
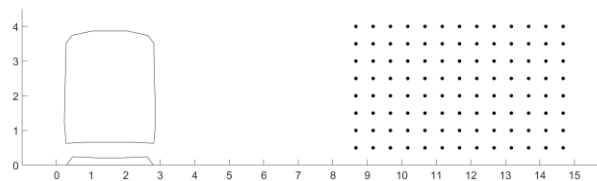

Figure 8 - Representation of the receiver grid used in the simulations.

6   Results

Initially, the acoustic performance of a purely reflective vertical barrier 1.20 m high and 0.15 m thick was evaluated. In Figure 9 the sound pressure levels for the scenarios with and without barrier (see Figure 9-a) to f)), and the IL (see Figure 9-g),h),i))), for three different frequencies: 500 Hz, 2000 Hz and 4000 Hz are presented. From the analysis of the Figure it is observed that there are relevant differences between the scenario without barrier and the scenario with barrier, which means that the barrier prevents the propagation of part of the energy. This phenomenon is even more remarkable when analysing the IL (see Figure 9-g),h),i))), where it is observed that the reduction (warmer colors of the figures) is higher than 15 dB.
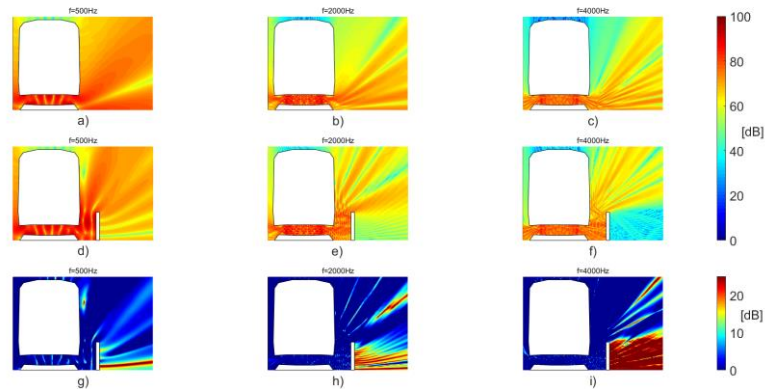
Figure 9 - Results calculated without (a,b,c) and with (d,e,f) the noise barrier, and the insertion loss (g,h,i), for vertical barrier.

The second phase of the study involved analyzing the proposed curved geometry. In Figure 10 the calculated results for the new barrier shape are illustrated. This figure is divided into three parts, illustrating the propagation in the case without barrier in Figure 10-a),b),c) , the scenario with the presence of the barrier, in Figure 10-d),e),f) and finally the insertion loss in Figure 10-g),h),i). In the case of the curved barrier, the attenuation effect is very clear, with reductions of over 15 dB.

Compared to the vertical barrier, the insertion loss presented by the curved barrier is higher. The phenomenon is again observed in the warmer colors that make up the color insertion loss map of the barrier under analysis.

The use of the track as a means of absorption plays an important role here, since part of the performance improvement is due to the characteristics of the ballast that absorbs the energy reflected on the inner surface of the curved barrier.
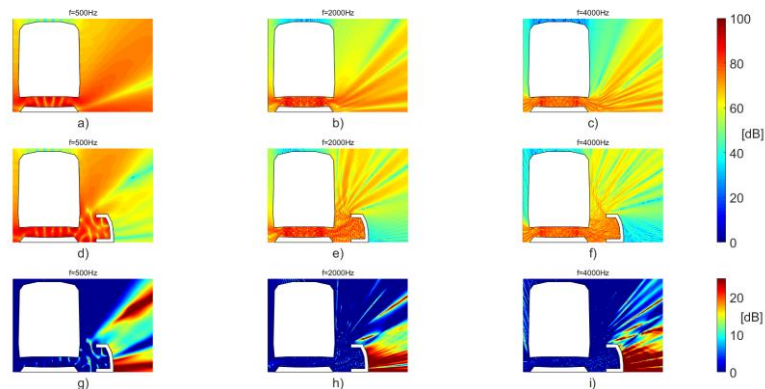

Figure 10 - Results calculated without (a,b,c) and with (d,e,f) the noise barrier, and the insertion loss (g,h,i), for curved barrier.

From the comparison between the vertical barrier and the curved barrier it can be concluded that the curved barrier is noticeably better at reducing sound pressure levels in the vicinity of the noise source, in particular for the lower frequencies. However, the secondary reflections that occur between the barrier and the vehicle are not properly attenuated and part of the energy is sent back to the external receivers.

Thus, an absorptive treatment was adopted on the inner face of the barrier to reduce the sound pressure level between the train box, the track and the acoustic barrier. Placing material with sound absorbing characteristics on the barriers ensures an improvement in acoustic performance, particularly with respect to the phenomenon mentioned above.

For this purpose, porous concrete was chosen due to its greater durability and excellent acoustic properties. The Figure 11 shows the geometry of the curved barrier filled by porous material, with an irregular geometry, to increase the absorbent surface. The geometry of the porous material shown is composed of two parts, namely a regular layer with a thickness of 0.08 m and an irregular layer. The irregular layer is composed of elements 0.06m thick and 0.10m wide, with equal spacing between them.
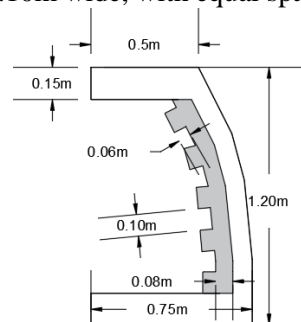

Figure 11 - Sound absorptive and curved noise barrier.

In Figure 12 the insertion loss calculated at the level of the receivers shown in Figure 8 can be seen. For this purpose, the energetic averaging of the sound pressure at the receivers was done for the cases with and without barrier and the insertion loss was then calculated.

With respect to the vertical barrier, the analysis shown in Figure 12 corroborates what has already been observed in the proximity to the noise source. The curved barrier performs substantially better than the vertical one, particularly from the frequency 630 Hz onwards. From 200 Hz to 630 Hz the insertion loss varies and the vertical barrier is slightly superior at some frequencies. From 630 Hz onwards, the insertion loss of the curved barrier stabilizes and the difference between the two is always more than 5 dB.

As far as the barrier with porous material is concerned it performs better compared to the purely reflective barriers for the entire frequency range under analysis. The performance of the curved barrier with porous material translates into an insertion loss of more than 10 dB over the entire frequency range, reaching 15 dB at most frequencies and for the frequency of 3150 Hz the insertion loss exceeds 25 dB.

In summary, for the lowest frequencies (200 Hz - 630 Hz), the difference between the three elements under study is not more than 2 to 3 dB; however, from 630 Hz on, the performance of the curved barrier with porous material is clearly superior compared to the other solutions presented.
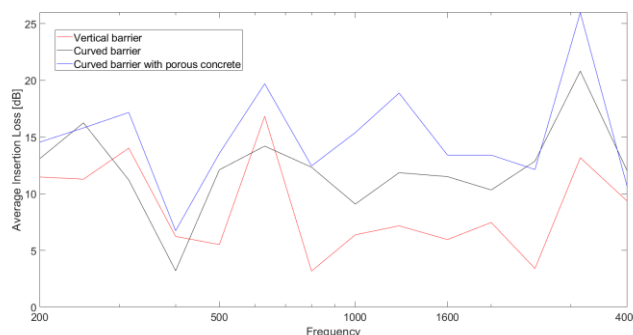

Figure 12 – Insertion loss calculated for the three proposed noise barrier.

Next, the IL color maps for the central frequencies of the one-third octave bands of 315 Hz, 1000 Hz, 1600 Hz and 2500 Hz are shown in Figure 13 for the curved barrier scenario with porous material. By analyzing the IL maps one can see that the influence of the barrier on the more distant receivers is very relevant, namely for the higher frequency bands. It should also be noted that, in the examples presented, the shadow zone of the barrier increases its influence in height as one moves away from the barrier. According to these results, receivers placed higher and further away from the barrier still exhibit a good level of protection. The color maps presented corroborate the average IL presented in Figure 12.
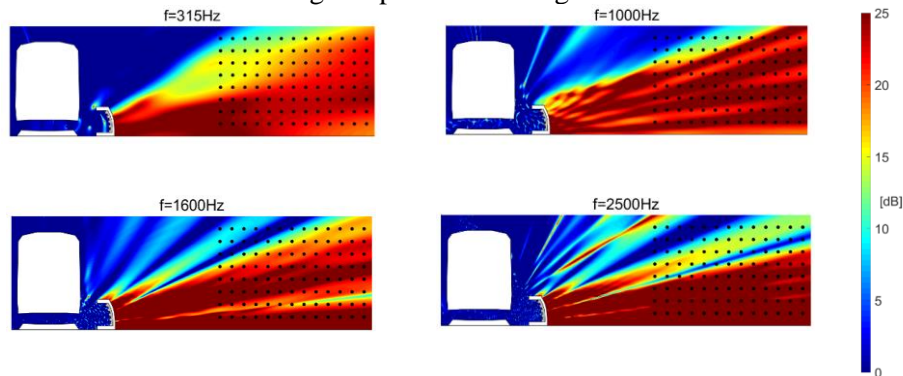

Figure 13 - Insertion loss maps for the curved noise barrier with absorptive layer for frequencies 315 Hz, 1000 Hz, 1600 Hz and 2500 Hz, with the presence of the receivers (black dots) used to calculate mean IL.

7 Conclusions

This paper summarizes the development of a low height acoustic barrier for use near the noise source in a railway environment. The development of the solution is composed of two distinct phases, namely the optimization of the barrier geometry and the integration of a porous material in order to increase the acoustic performance of the solution. Using the sound pressure level records acquired in the railway environment in the metropolitan area of Porto, it was possible to define the most important frequency content and thus design a solution whose performance was superior in that frequency range. The numerical modelling and the study of the various solutions was done by applying a multi-region BEM formulation. The parametric study presents the methodology for the sizing of the curved barrier. Through the simulation of a sound wave, the inner face of the barrier was constructed to coincide with the shape of the incident wave front. In this way normal reflection is favoured and, as such, more energy is sent in the direction of the noise source.

The methodology adopted intends to create an integrated solution taking advantage of the acoustic absorption capacity of the track to absorb the energy sent back. In a complementary way, a porous concrete layer was added, which on the one hand has a good acoustic absorption capacity and, on the other hand, guarantees the durability required for solutions used outdoors.

The main purpose of the porous material is to absorb part of the energy resulting from reflections between the barrier and the vehicle, ensuring that the energy is not sent to the receivers. The results presented show the clear improvement achieved by using porous material as a means of absorbing some of the energy over purely reflective solutions.

The curved solution with porous material presents an IL at the defined receivers higher than 10 dB throughout the calculated frequency range, with peaks higher than 15 dB at some frequencies.

The presented solution proves to be an element capable of reducing the train-induced noise with great effectiveness. Due to its low height, this solution does not represent a visual obstacle, as is usual for noise barriers, meeting the final objective.

Acknowledgements

8 References

[1] European Environment Agency, "Environmental noise in Europe - 2020," European Environment Agency (EEA), 2019. [Online]. Available: https://www.eea.europa.eu/publications/environmental-noise-in-europe

[2] N. Blanes, A. Marín, and M. J. Ramos, "Noise exposure scenarios in 2020 and 2030 outlooks for EU 28," European Environment Agency, 978-82-93752-02-8, 2019. [Online]. Available: https://www.eionet.europa.eu/etcs/etc-atni

[3] P. De Vos, "Railway noise in Europe. State of the art report," International Union of Railways (UIC), 2016, vol. 118.

[4] !!! INVALID CITATION !!! [4-6].

[5] D. Thompson, *Railway noise and vibration: mechanisms, modelling and means of control*. Elsevier, 2008.

[6] A. Jolibois, J. Defrance, H. Koreneff, P. Jean, D. Duhamel, and V. W. Sparrow, "In situ measurement of the acoustic performance of a full scale tramway low height noise barrier prototype," *Applied Acoustics,* vol. 94, pp. 57-68, 2015.

[7] F. Koussa, J. Defrance, P. Jean, and P. Blanc-Benon, "Acoustic performance of gabions noise barriers: numerical and experimental approaches," *Applied acoustics,* vol. 74, no. 1, pp. 189-197, 2013.

[8] R. Bartolini, S. Filippozzi, E. Princi, C. Schenone, and S. Vicini, "Acoustic and mechanical properties of expanded clay granulates consolidated by epoxy resin," *Applied Clay Science,* vol. 48, no. 3, pp. 460-465, 2010.

[9] J. Carbajo San Martín, T. V. Esquerdo-Lloret, J. Ramis-Soriano, A. V. Nadal-Gisbert, and F. D. Denia, "Acoustic properties of porous concrete made from arlite and vermiculite lightweight aggregates," 2015.

[10] T. S. Tie, K. H. Mo, A. Putra, S. C. Loo, U. J. Alengaram, and T.-C. Ling, "Sound absorption performance of modified concrete: A review," *Journal of Building Engineering,* vol. 30, p. 101219, 2020/07/01/ 2020, doi: https://doi.org/10.1016/j.jobe.2020.101219.

[11] M. J. Crocker, *Handbook of noise and vibration control*. John Wiley & Sons, 2007.

[12] S. M. Kirkup, *The boundary element method in acoustics*. Integrated sound software, 2007.

[13] *Acoustics — Determination of sound absorption coefficient and impedance in impedance tubes — Part 2: Transfer-function method*, International Organization for Standardization, 1998.

[14] H. Utsuno, T. Tanaka, T. Fujikawa, and A. Seybert, "Transfer function method for measuring characteristic impedance and propagation constant of porous materials," *The Journal of the Acoustical Society of America,* vol. 86, no. 2, pp. 637-643, 1989.

[15] M. Pereira, J. Carbajo, L. Godinho, J. Ramis, and P. Amado-Mendes, "Improving the sound absorption behaviour of porous concrete using embedded resonant structures," *Journal of Building Engineering,* vol. 35, p. 102015, 2021.

[16] S. Marburg and B. Nolte, *Computational acoustics of noise propagation in fluids: finite and boundary element methods*. Springer, 2008.

[17] A. Seybert, C. Cheng, and T. Wu, "The solution of coupled interior/exterior acoustic problems using the boundary element method," *The Journal of the Acoustical Society of America,* vol. 88, no. 3, pp. 1612-1618, 1990.

[18] R. Broadbent, D. Thompson, and C. Jones, "The acoustic properties of railway ballast," 2009.